

Figure 2. Bond lengths in the metallacyclopentane rings. The reported values are distances (Å) corrected for libration motion about the metal atom (see text).

distances in the iridiacycle do not allow one to be positive in this case. It may also be interesting to note that in **6** C(1)-C(2) is probably shorter than C(3)-C(4), their difference being equal to 2.6σ . In principle, one cannot rule out the possibility that some of the observed shortening effect is an artifact created by the thermal motion of the carbon atoms in the rings. However, the results of a thermal motion analysis, performed by assuming a rigid-body libration about the metal atom,³⁴ left no doubts about the occurrence of the asymmetric C-C distance sequence in the rhodiacycle and about the reality of the other peculiar features of these cycles, at least in the case of **1** and **6** (Figure 2). In fact, in view of the possible torsional oscillations, suggested by the shape of the relevant thermal ellipsoids (Figure 1) and not taken into account by the assumed thermal motion model, the C(2)-C(3) bond lengths reported in Figure 2 should be considered as lower limits to the "true" values; nevertheless the fact that the relevant thermal parameters (Table III) are not unusually large and that, after the correction for rigid-body libration,

C(2)-C(3) is still significantly smaller than the adjacent C-C bonds indicates that these additional shortening effects cannot be large enough to justify the observed differences.

Even though the present evidence suggests, at least for the cobalt triad, a possible role of the metal in determining the C-C distance sequence in the metallacyclic rings (complexes **1** and **4** are isostructural, the only difference being the nature of the metal), the available data do not allow us to establish any clear correlation supporting this suggestion.

We would also like to point out the possible relevance of these findings to the carbon-carbon and carbon-hydrogen soft activation via transition-metal alkyls.

Acknowledgment. We thank CNR (Rome) for financial support and the "Centro CNR per le Macromolecole Stereoordinate ed Otticamente Attive" (Pisa) for use of their NMR and MS facilities.

Registry No. **1**, 63162-06-1; **2**, 63162-03-8; **3**, 63162-04-9; **4**, 66416-07-7; **5**, 74562-96-2; **6**, 74562-97-3; **7**, 63179-49-7; **8**, 32761-86-7; **9**, 66517-28-0; **10**, 42920-62-7; **11**, 23708-47-6; **12**, 23708-48-7; **13**, 17036-36-1; **14**, 2123-72-0; **15**, 26198-40-3; (η^5 -C₅Me₅)RhBr₂(PPh₃), 63179-48-6; (η^5 -C₅Me₅)IrBr₂(PPh₃), 74562-98-4; *n*-pentane, 109-66-0; 1-pentene, 109-67-1; *cis*-2-pentene, 627-20-3; *trans*-2-pentene, 646-04-8; 1-hexene, 592-41-6; *cis*-2-hexene, 7688-21-3; *n*-hexane, 110-54-3; *cis*-3-hexene, 7642-09-3; *trans*-3-hexene, 13269-52-8; *trans*-2-hexene, 4050-45-7; *n*-butane, 106-97-8; 1-butene, 106-98-9; 1,5-dibromopentane, 111-24-0; 1,6-dibromohexane, 629-03-8; 1,4-dibromobutane, 110-52-1.

Supplementary Material Available: Listings of the observed and calculated structure factors and of the C-C(phenyl) distances for the three structures (85 pages). Ordering information is given on any current masthead page.

Contribution from the Department of Chemistry,
University of New Mexico, Albuquerque, New Mexico 87131

Reactions of Aminophosphines with Carbon Dioxide, Carbonyl Sulfide, and Carbon Disulfide. Crystal and Molecular Structure of a Seven-Coordinate Tris(dithiocarbamato) Complex of Phosphorus(III)

R. W. LIGHT, L. D. HUTCHINS, R. T. PAINE,* and C. F. CAMPANA*

Received April 2, 1980

The room-temperature reactions of the aminophosphines [(CH₃)₂N]₃P, [(CH₃)₂N]₂PCl, [(CH₃)₂N]₂PF, (CH₃)₂NPCl₂, (CH₃)₂NPF₂, CH₃NCH₂CH₂N(CH₃)PCl, and CH₃NCH₂CH₂N(CH₃)PF with CO₂, COS, and CS₂ have been investigated. Several reactions proceed to products in which CO₂, COS, or CS₂ have undergone insertion in the P-N bonds. The products have been systematically characterized by mass, infrared, and multinuclear NMR spectrometries. The insertion product with the empirical molecular formula [(CH₃)₂N]₃P·3CS₂ has also been subjected to single-crystal X-ray structural analysis. The complex crystallizes in the monoclinic space group P2₁/n with *a* = 7.180 (1) Å, *b* = 30.907 (6) Å, *c* = 16.300 (4) Å, β = 91.20 (2)°, *Z* = 8, *V* = 3616.4 (1) Å³ and ρ = 1.44 g cm⁻³. Diffraction data were collected with a Syntex P3/F automated diffractometer using Mo K α radiation. The structure was solved by using MULTAN, and the full-matrix least-squares refinement converged with final discrepancy indices *R*_F = 0.066 and *R*_{wF} = 0.0101 on 4764 independent reflections. The crystals contain the discrete monomeric P-N bond insertion product tris(dithiocarbamato)phosphorus(III) [P(S₂CN(CH₃)₂)₃]. The compound is formally seven-coordinate with the six sulfur atoms and the phosphorus atom lone pair forming a distorted capped trigonal antiprism. The PS₆ core has three short P-S bond lengths, 2.162 (3)-2.202 (3) Å, and three long P-S bond lengths, 2.873 (3)-3.016 (3) Å, with one short and one long P-S bond length associated with each planar dithiocarbamate ligand.

Introduction

The interactions of transition-metal complexes with small molecules such as N₂, O₂, NO, CO, CO₂, and SO₂ have recently attracted attention particularly within the context of catalytic conversion chemistry.¹ We have had an interest in

the interactions of several small molecules with coordinatively unsaturated metal complexes stabilized by multifunctional aminophosphines, and in the course of our work^{2,3} we have found it necessary to obtain a better understanding of the

(1) A survey of small-molecule activation chemistry and catalysis appears in: Kahn, M. M. T.; Martell, A. E. "Homogeneous Catalysis by Metal Complexes"; Academic Press: New York, 1974; Vol. I.

(2) Light, R. W.; Paine, R. T. *Phosphorus Sulfur*, in press.

(3) A preliminary report on our results was presented earlier: Light, R. W.; Paine, R. T. "Abstracts of Papers", 34th Southwest Regional Meeting of the American Chemical Society, Corpus Christi, TX, 1978; American Chemical Society: Washington DC, 1978; INOR 7.

reactions of CO₂, COS, CS₂, and SO₂ with uncomplexed aminophosphines. The multiple reaction sites present in aminophosphines suggest that combinations of these ligands with CO₂, COS, or CS₂ could result in the formation of several classes of compounds including oxidation products, simple addition complexes, phosphonium salts, or P–N bond insertion products having monodentate or bidentate coordination modes at the phosphorus atom. Results from earlier studies^{4–8} confirm several of these expectations. For example, in 1898 Michaelis proposed the formation of a monodentate dithiocarbamate insertion product, PhP[SC(S)pip]₂, from the combination of CS₂ and bis(piperidyl)phenylphosphine.⁴ More recently, the reactions of several aminophosphines including (R₂N)₃P (R = Me, Et, Pr, Bu),^{5,7} EtP(NMe₂)₂,⁷ MeP(NMe₂)₂,^{6,7} Me₂P(NMe₂)₂,⁷ and Ph₂P(NMe₂)₂⁷ with CS₂ have been reported. In each case CS₂ was readily absorbed by the ligand, and with [(CH₃)₂N]₃P a red solution developed whose color faded rapidly at 25 °C. The transient red species was assumed to be a phosphonium salt, [(Me₂N)₃P⁺][CS₂[−]], on the basis of infrared and ¹H NMR data^{5–8} and an expected structural analogy with [Et₃P⁺][CS₂[−]].⁹ The characterization data for the final colorless products were interpreted in favor of the formation of monodentate dithiocarbamate products.^{5–8} Related reactions of several aminoarsines with CS₂ have been reported, and (monodentate dithiocarbamate)arsenic(III) derivatives were proposed as products.^{10,11} However, a brief description of a single-crystal X-ray diffraction analysis for one compound [(C₂H₅)₂NCS₂]₃As revealed an unexpected AsS₆ coordination sphere formed by three asymmetric bidentate dithiocarbamate ligands.¹²

Considerably less is known about the reactions of CO₂ and COS with aminophosphines. Holtschmidt and co-workers⁶ reported that ligands of the types (R₂N)₃P, RP(NR₂)₂, (RO)₂PNR₂, and ROP(NR₂)₂ (R = alkyl) in combination with CO₂ form monodentate carbamate insertion complexes. However, the structural proposals were not supported by detailed spectroscopic analyses. Moore and Yoder¹³ have also reported the formation of monodentate S-bonded thio-carbamate complexes from mixtures of COS and a series of aminoalkylphosphines. The molecular structures of the P–N bond insertion derivatives also have not been unambiguously confirmed. Lastly, Cavell and co-workers¹⁴ have observed that the P–N bond in the phosphorane CH₃(CF₃)₃PN(CH₃)₂ is subject to insertion by CO₂, COS, and CS₂. A single-crystal X-ray analysis for CH₃(CF₃)₃P[O₂CN(CH₃)₂] revealed the formation of a six-coordinate phosphorane having a bidentate carbamate ligand.

It is apparent that the P–N bond insertion products described in these earlier studies remain open to further spectroscopic and structural characterization. In this paper we report investigations of the reactions of several important aminophosphines with CO₂, COS, and CS₂. Detailed spectroscopic analyses of the structures of the products are described, and a reinvestigation of the chemistry and structure of the complex having the empirical composition [(CH₃)₂N]₃P·3CS₂ is presented.

Experimental Section

General Information. Standard high-vacuum and inert-atmosphere synthetic techniques were used for the manipulations of all reagents and reaction products. Mass spectra were recorded on a Du Pont Model 21-491 spectrometer operating at 70 eV with an inlet temperature of 30 °C and a source temperature of 100 °C. Samples (solids and liquids) were introduced through a heated-solids probe. Infrared spectra were recorded on a Perkin-Elmer Model 621 spectrometer. The samples were investigated as liquids or solutions between KBr plates or as KBr pellets. The spectra were calibrated with polystyrene film absorptions. The NMR spectra were recorded on a Varian XL-100 NMR spectrometer operating at 25.2 MHz (¹³C), 40.5 MHz (³¹P), 94.1 MHz (¹⁹F), and 100 MHz (¹H). The data were collected in the pulse mode with use of a Nicolet TT 100 data system. Samples were contained in sealed 5-mm tubes rigidly placed in a 12-mm tube containing a deuterated lock solvent. Spectra standards were (CH₃)₄Si (¹³C, ¹H), 85% H₃PO₄ (³¹P), and CFCl₃ (¹⁹F).

Materials. The aminophosphine ligands were prepared by standard literature methods.¹⁵ CO₂ and COS were obtained from Matheson Co., and they were purified by trap to trap distillations. CS₂ was obtained from Mallinckrodt Chemical Co., and it was dried over molecular sieves and vacuum distilled. The common organic solvents employed here were dried by accepted procedures and degassed by repeated freeze–thaw cycles. All solvent transfers were accomplished by vacuum distillation.

Preparation of [(CH₃)₂N]₂POC(O)N(CH₃)₂ (1). Typically, 1.2 mmol of [(CH₃)₂N]₃P was syringed into a 25-mL Schlenk flask under a nitrogen atmosphere. The flask was frozen and evacuated, and 1.2 mmol of carbon dioxide was condensed onto the ligand. The contents were warmed to 25 °C and stirred for 12 h. The volatile products were vacuum evaporated, and the product 1 was recovered as a colorless oil in 80% yield.¹⁶

Preparation of (CH₃)₂NP[OC(O)N(CH₃)₂]₂ (2). Typically, 6.1 mmol of [(CH₃)₂N]₃P was syringed into a 50-mL Kel-F reaction tube under a nitrogen atmosphere. The tube was attached to a metal vacuum line through a high-pressure metal valve. The contents were degassed by repeated freeze–thaw cycles and then exposed to excess CO₂ at 1500 torr and 25 °C for 2 weeks. The excess CO₂ was then evacuated, and the remaining oil was collected under a nitrogen atmosphere in 90% yield.¹⁶

Preparation of (CH₃)₂N(F)P[OC(O)N(CH₃)₂]₂ (3). Typically, 1.4 mmol of FP[N(CH₃)₂]₂ was syringed into a 25-mL Schlenk tube under a nitrogen atmosphere. The flask was frozen and evacuated, and 2.0 mmol of CO₂ was condensed onto the ligand. The contents were warmed to 25 °C and stirred for 30 min. Excess CO₂ was evacuated, and a colorless oil was recovered with about 95% yield. The product is unstable at 25 °C in the absence of excess CO₂.

Preparation of (CH₃)₂NP[SC(O)N(CH₃)₂]₂ (4). Typically, 3.0 mmol of [(CH₃)₂N]₃P was syringed into a 50-mL Schlenk flask under a nitrogen atmosphere. The flask was frozen and evacuated, and exposed to excess gaseous COS (600 torr) at 25 °C for 3 h. The volatile products were evacuated leaving a white solid product in 85% yield.¹⁶

Preparation of (CH₃)₂NP[SC(S)N(CH₃)₂]₂ (5). Typically, 2.0 mmol of [(CH₃)₂N]₃P was syringed into a 50-mL Schlenk flask, and a solution containing 4.0 mmol CS₂ in CHCl₃ was added. The mixture was stirred at 25 °C for 6 h, and the slightly yellow solid product was recovered after vacuum evaporation of the volatile reagents. The product yield was 95%.¹⁶

Preparation of P[S₂CN(CH₃)₂]₃ (6). Typically this was obtained by refluxing P[N(CH₃)₂]₃ in excess, dry CS₂ for 24 h. The solid product (95% yield) was collected by filtration under dry nitrogen, washed with diethyl ether, and stored under dry nitrogen.¹⁶

Miscellaneous Reactions. [(CH₃)₂N]₃P was exposed to excess CO₂ at 1500 torr and 25 °C for 24 h. Complex 2 was isolated in high yield, and no evidence for the formation of the tris-insertion product [(C-H₃)₂NC(O)O]₃P was found. Under a wide range of conditions and stoichiometries, FP[N(CH₃)₂]₂ and [(CH₃)₂N]₃P were combined with

- (4) Michaelis, A. *Chem. Ber.* **1898**, *31*, 1037.
- (5) Vetter, H. J.; Nöth, H. *Chem. Ber.* **1963**, *96*, 1308.
- (6) Oertel, G.; Mally, H.; Holtschmidt, H. *Chem. Ber.* **1963**, *97*, 891.
- (7) Jensen, K. A.; Dahl, O.; Henriksen, L. E. *Acta Chem. Scand.* **1970**, *24*, 1179.
- (8) Cragg, R. H.; Lappert, M. F. *J. Chem. Soc. A* **1966**, 82.
- (9) Margulis, T. N.; Templeton, D. J. *J. Am. Chem. Soc.* **1961**, *83*, 995.
- (10) Malatesta, L. *Gazz. Chim. Ital.* **1939**, *69*, 629.
- (11) Chatt, J.; Duncanson, L. A.; Venanzi, L. M. *Suom. Kemistil. B* **1956**, *29B*, 75.
- (12) Colapietro, M.; Domenicano, A.; Scaramuzza, L.; Vacicagi, A. *Chem. Commun.* **1968**, 302.
- (13) Moore, W. S.; Yoder, C. H. *J. Organomet. Chem.* **1975**, *87*, 389.
- (14) The, K. I.; Vande Griend, L.; Whitla, W. A.; Cavell, R. G. *J. Am. Chem. Soc.* **1977**, *99*, 7379.

- (15) (a) Burg, A. B.; Slota, P. J. *J. Am. Chem. Soc.* **1958**, *80*, 1107. (b) Fleming, S.; Parry, R. W. *Inorg. Chem.* **1972**, *11*, 1. (c) Fleming, S.; Lupton, M. K.; Jekot, K. *Ibid.* **1972**, *11*, 2534. (d) Fleming, S. Ph.D. Thesis, University of Michigan, Ann Arbor, MI, 1962.
- (16) Elemental analyses were consistent with the formulations for the compounds. Tables of mass, infrared and NMR spectroscopic data are available as supplementary material.

Table I. Experimental Data for the X-ray Diffraction Study on Crystalline $P[S_2CN(CH_3)_2]_3$

(A) Crystal Parameters at 27 °C	
crystal system: monoclinic	$V = 3616.4 (1) \text{ \AA}^3$
space group: $P2_1/n$	$Z = 8$
$a = 7.180 (1) \text{ \AA}$	mol wt = 391.6
$b = 30.907 (6) \text{ \AA}$	$F(000) = 1632.0$
$c = 16.300 (4) \text{ \AA}$	$\rho(\text{calcd}) = 1.44 \text{ g cm}^{-3}$
$\beta = 91.20 (2)^\circ$	
(B) Measurement of Intensity Data	
diffractometer: Syntex P3/F	
radiation: Mo $K\alpha$ ($\lambda = 0.71069 \text{ \AA}$)	
monochromator: highly oriented graphite crystal	
reflections measd: $+h, +k, \pm l$	
2θ range: $3\text{--}45^\circ$	
scan type: $\theta\text{--}2\theta$	
scan speed: $3.91\text{--}29.3^\circ/\text{min}$	
scan range: from $[2\theta(K\alpha_1) - 1.0]^\circ$ to $[2\theta(K\alpha_2) + 1.0]^\circ$	
bkgd measmt: stationary-crystal counter; at beginning and end of 2θ scan—each for half the time taken for 2θ scan	
std refltns: 2 measd every 48 refltns [153; 342]	
refltns collected: 5336 total, yielding 4764 independent refltns	
refltns obsd ($I \geq 2\sigma_I$): 3515 (74%)	
abs coeff: 8.1 cm^{-1}	

COS; however, only **4** was isolated from the reaction of $[(CH_3)_2N]_3P$ with COS. Excess CO_2 , COS, and CS_2 were found to be unreactive toward $CIP[N(CH_3)_2]_2$, $Cl_2PN(CH_3)_2$, $F_2PN(CH_3)_2$, and $CH_3N-CH_2CH_2N(CH_3)PF$ on the basis of ^{31}P NMR spectra. Attempts to prepare the mono-insertion products $[(CH_3)_2N]_2PCS(S)N(CH_3)_2$ and $(CH_3)_2NP(F)SC(S)N(CH_3)_2$ by careful reactant stoichiometry regulation led only to the formation of **5** and **6**, respectively.

Crystal Structure Determination of $P[S_2CN(CH_3)_2]_3$. The crystal used in the structure determination was obtained directly from the preparation of **6**. A crystal $0.38 \text{ mm} \times 0.12 \text{ mm} \times 0.38 \text{ mm}$ was lodged in a glass capillary and sealed under dry nitrogen. The crystal was centered on a Syntex P3/F automated diffractometer, and the determinations of the crystal class, the orientation matrix, and accurate unit cell parameters were performed in a standard manner.¹⁷ The data were collected at 298 K by the $\theta\text{--}2\theta$ technique using Mo $K\alpha$ radiation, a scintillation counter, and pulse-height analyzer. Details of the data collection are summarized in Table I. Inspection of the collected data revealed systematic absences $h + l = 2n + 1$ for $h0l$ and $k = 2n + 1$ for $0k0$, and the monoclinic space group $P2_1/n$ was indicated. Corrections for absorption were found to be unnecessary. The redundant and equivalent reflection data were averaged and converted to unscaled $|F_o|$ values following corrections for Lorentz and polarization effects.

Solution and Refinement of the Structure. Initial calculations were carried out on a Syntex R3/XTL structure determination system.¹⁷ Scattering factors for P, S, N, and C atoms were taken from the compilation of Cromer and Weber,¹⁸ while those for hydrogen were taken from Stewart and co-workers.¹⁹ Both real ($\Delta f'$) and imaginary ($\Delta f''$) components of the anomalous dispersion were included for the P and S atoms by using the values listed by Cromer and Liberman.²⁰ The function minimized during the least-squares refinement was $\sum w(|F_o| - |F_c|)^2$.²¹

Table II. Positional Parameters and Their Esd's for $P[S_2CN(CH_3)_2]_3$

atom	x/a	y/b	z/c
Molecule A			
P(1)	0.7892 (3)	0.33901 (7)	0.1887 (1)
S(1A)	0.8075 (3)	0.39733 (7)	0.2660 (1)
S(1B)	0.7234 (3)	0.31983 (7)	0.3672 (1)
S(2A)	1.0808 (3)	0.32336 (7)	0.2146 (1)
S(2B)	0.8891 (4)	0.26143 (8)	0.1030 (2)
S(3A)	0.8648 (3)	0.37760 (8)	0.0839 (1)
S(3B)	0.4542 (3)	0.37258 (9)	0.1042 (1)
N(1)	0.7639 (9)	0.3998 (2)	0.4243 (4)
N(2)	1.2272 (10)	0.2493 (2)	0.1686 (4)
N(3)	0.6220 (12)	0.4199 (3)	-0.0090 (4)
C(1)	0.7642 (10)	0.3731 (3)	0.3609 (5)
C(2)	1.0770 (12)	0.2741 (3)	0.1608 (4)
C(3)	0.6336 (12)	0.3927 (3)	0.0552 (5)
C(1A)	0.7378 (13)	0.3831 (3)	0.5075 (5)
C(1B)	0.7942 (15)	0.4466 (3)	0.4167 (6)
C(2A)	1.3887 (13)	0.2610 (4)	0.2213 (7)
C(2B)	1.2410 (13)	0.2097 (3)	0.1210 (6)
C(3A)	0.7849 (17)	0.4372 (4)	-0.0510 (6)
C(3B)	0.4455 (17)	0.4360 (4)	-0.0349 (6)
H(1A1)	0.6442	0.3600	0.5060
H(1A2)	0.8562	0.3715	0.5290
H(1A3)	0.6960	0.4065	0.5431
H(1B1)	0.8817	0.4562	0.4600
H(1B2)	0.8457	0.4530	0.3630
H(1B3)	0.6754	0.4617	0.4225
H(2A1)	1.3457	0.2765	0.2698
H(2A2)	1.4544	0.2346	0.2388
H(2A3)	1.4736	0.2795	0.1908
H(2B1)	1.1656	0.1870	0.1462
H(2B2)	1.1949	0.2148	0.0647
H(2B3)	1.3712	0.2002	0.1196
H(3A1)	0.8740	0.4488	-0.0102
H(3A2)	0.8443	0.4141	-0.0821
H(3A3)	0.7452	0.4604	-0.0884
H(3B1)	0.3468	0.4177	-0.0122
H(3B2)	0.4304	0.4657	-0.0155
H(3B3)	0.4357	0.4354	-0.0950
Molecule B			
P(1')	0.7292 (3)	0.09096 (7)	0.2154 (1)
S(1A')	0.7066 (3)	0.14037 (7)	0.1203 (1)
S(1B')	0.7878 (3)	0.05463 (8)	0.0463 (1)
S(2A')	0.4401 (3)	0.07186 (8)	0.1969 (1)
S(2B')	0.6346 (3)	0.01400 (8)	0.3168 (1)
S(3A')	0.6490 (3)	0.13724 (8)	0.3081 (1)
S(3B')	1.0584 (3)	0.1378 (2)	0.2845 (2)
N(1')	0.7540 (9)	0.1280 (2)	-0.0370 (4)
N(2')	0.2911 (9)	0.0017 (2)	0.2552 (4)
N(3')	0.8830 (12)	0.1852 (3)	0.3943 (5)
C(1')	0.7511 (10)	0.1074 (3)	0.0339 (5)
C(2')	0.4469 (11)	0.0254 (3)	0.2586 (5)
C(3')	0.8743 (13)	0.1570 (3)	0.3327 (5)
C(1A')	0.7247 (13)	0.1749 (3)	-0.0459 (5)
C(1B')	0.7826 (12)	0.1043 (3)	-0.1134 (5)
C(2A')	0.1319 (13)	0.0122 (3)	0.2056 (7)
C(2B')	0.2730 (14)	-0.0373 (3)	0.3072 (5)
C(3A')	0.7178 (18)	0.1990 (4)	0.4387 (7)
C(3B')	1.0551 (19)	0.2061 (4)	0.4193 (7)
H(1A1')	0.6598	0.1809	-0.0981
H(1A2')	0.6491	0.1854	-0.0005
H(1A3')	0.8452	0.1898	-0.0446
H(1B1')	0.8383	0.0760	-0.1010
H(1B2')	0.6626	0.1001	-0.1421
H(1B3')	0.8661	0.1208	-0.1486
H(2A1')	0.1489	0.0012	0.1498
H(2A2')	0.0208	-0.0011	0.2288
H(2A3')	0.1156	0.0437	0.2037
H(2B1')	0.3245	-0.0315	0.3622
H(2B2')	0.1408	-0.0450	0.3111
H(2B3')	0.3406	-0.0614	0.2825
H(3A1')	0.7554	0.2181	0.4842
H(3A2')	0.6333	0.2147	0.4012
H(3A3')	0.6540	0.1736	0.4604
H(3B1')	1.0483	0.2150	0.4770
H(3B2')	1.1594	0.1861	0.4128
H(3B3')	1.0746	0.2319	0.3852

(17) Hardware configuration for the P3/F diffractometer and the R3/XTL system has been described: Campana, C. F.; Sheppard, D. F.; Litchman, W. M. *Inorg. Chem.*, in press. Programs used for centering of reflections, autoindexing, refinement of cell parameters, axial photographs, data collection, data reduction, Fourier syntheses, block-diagonal and full-matrix least-squares refinement, bond-length and bond-angle calculations, error analysis, least-squares planes calculations, direct-methods structure solution, and calculation of hydrogen atom positions are those described in: Sparks, R. A., Ed. "Syntex R3 Operations Manual"; Syntex Analytical Instruments: Cupertino, CA, 1978.

(18) Cromer, D. T.; Weber, J. T. *Acta Crystallogr., Sect. B* **1965**, *B18*, 104.

(19) Stewart, R. F.; Davidson, R. F.; Simpson, W. T. *J. Chem. Phys.* **1965**, *42*, 3175.

(20) Cromer, D. T.; Liberman, D. J. *J. Chem. Phys.* **1970**, *53*, 1891.

(21) Discrepancy indices used in the text are defined as follows: $R_p(\%) = [\sum |F_o| - |F_c|] / [\sum |F_o|] \times 100$, $R_w(\%) = [\sum w(|F_o| - |F_c|)^2 / \sum w|F_o|^2]^{1/2} \times 100$. The "goodness of fit" (GOF) is defined as $GOF = [\sum w(|F_o| - |F_c|)^2 / (NO - NV)]^{1/2}$, wherein NO is the number of observations and NV is the number of variables.

Table III. Thermal Parameters ($\times 100$)^a and Their Esd's for $\text{P}[\text{S}_2\text{CN}(\text{CH}_3)_2]_3$

atom	U_{11}	U_{22}	U_{33}	U_{12}	U_{13}	U_{23}
Molecule A						
P(1)	3.8 (1)	4.3 (1)	4.4 (1)	0.0 (1)	0.2 (1)	0.0 (1)
S(1A)	5.8 (1)	3.5 (1)	4.8 (1)	0.0 (1)	0.3 (1)	0.01 (9)
S(1B)	5.7 (1)	4.3 (1)	5.7 (1)	-0.1 (1)	0.3 (1)	0.4 (1)
S(2A)	3.6 (1)	5.0 (1)	5.4 (1)	0.1 (1)	-0.5 (1)	-1.3 (1)
S(2B)	6.4 (2)	5.5 (2)	7.3 (2)	-0.4 (1)	-0.9 (1)	-1.9 (1)
S(3A)	4.4 (1)	6.3 (2)	4.9 (1)	-0.1 (1)	0.6 (1)	0.8 (1)
S(3B)	4.3 (1)	6.9 (2)	6.5 (1)	0.6 (1)	0.8 (1)	0.3 (1)
N(1)	4.2 (4)	5.5 (5)	4.5 (4)	1.0 (3)	-0.9 (3)	-1.1 (3)
N(2)	5.4 (5)	4.5 (5)	6.3 (5)	1.6 (4)	1.4 (4)	-0.6 (4)
N(3)	7.5 (6)	6.6 (6)	4.6 (4)	0.8 (5)	-1.0 (4)	1.2 (4)
C(1)	3.1 (4)	3.9 (5)	4.4 (5)	0.6 (4)	0.0 (4)	0.2 (4)
C(2)	4.4 (5)	3.2 (6)	3.6 (4)	0.0 (4)	1.5 (4)	0.1 (4)
C(3)	3.9 (5)	5.2 (6)	4.7 (5)	0.6 (4)	0.8 (4)	-0.7 (4)
C(1A)	5.4 (6)	9.0 (8)	3.8 (5)	1.5 (5)	-0.4 (4)	-1.5 (5)
C(1B)	7.0 (7)	5.1 (6)	9.2 (7)	0.5 (5)	-0.8 (6)	-2.7 (5)
C(2A)	4.4 (6)	8.5 (9)	10.2 (8)	2.2 (6)	0.4 (6)	1.2 (6)
C(2B)	9.5 (8)	4.9 (7)	8.9 (7)	2.3 (6)	3.0 (7)	-0.6 (5)
C(3A)	10.3 (9)	9.6 (9)	5.0 (6)	-1.9 (7)	-0.3 (6)	2.9 (6)
C(3B)	9.2 (8)	7.3 (8)	6.7 (7)	2.6 (7)	-1.3 (6)	0.1 (6)
Molecule B						
P(1')	3.3 (1)	4.8 (1)	4.5 (1)	-0.3 (1)	0.1 (1)	0.4 (1)
S(1A')	5.0 (1)	3.8 (1)	4.6 (1)	0.0 (1)	0.5 (1)	0.31 (9)
S(1B')	6.3 (2)	3.9 (1)	6.5 (1)	0.3 (1)	0.2 (1)	0.2 (1)
S(2A')	3.4 (1)	5.7 (2)	6.1 (1)	-0.5 (1)	-0.5 (1)	1.6 (1)
S(2B')	4.9 (1)	5.9 (2)	5.5 (1)	-0.1 (1)	-0.9 (1)	1.1 (1)
S(3A')	4.5 (1)	6.0 (2)	5.6 (1)	0.2 (1)	0.7 (1)	-0.5 (1)
S(3B')	4.6 (1)	9.1 (2)	6.3 (1)	-1.1 (1)	0.2 (1)	-0.3 (1)
N(1')	3.4 (4)	4.3 (4)	5.1 (4)	-0.2 (3)	-0.2 (3)	0.0 (3)
N(2')	3.5 (4)	5.4 (5)	6.2 (4)	-0.5 (3)	0.5 (3)	-0.1 (4)
N(3')	8.0 (6)	5.4 (5)	5.6 (5)	-1.2 (4)	0.1 (4)	-0.6 (4)
C(1')	2.7 (4)	3.6 (5)	5.7 (5)	-0.8 (4)	-0.1 (4)	-0.5 (4)
C(2')	4.1 (5)	3.2 (5)	5.3 (5)	0.4 (4)	0.6 (4)	-0.6 (4)
C(3')	5.4 (6)	5.6 (6)	5.4 (5)	-0.2 (5)	-0.2 (5)	1.1 (5)
C(1A')	6.0 (6)	3.6 (5)	6.8 (6)	0.0 (4)	-0.2 (5)	0.7 (4)
C(1B')	4.4 (5)	7.6 (7)	4.1 (5)	-0.5 (5)	-0.3 (4)	-0.2 (4)
C(2A')	4.2 (6)	7.0 (8)	11.4 (9)	-0.7 (5)	1.0 (6)	-0.4 (6)
C(2B')	6.6 (6)	5.1 (6)	6.4 (6)	-1.4 (5)	1.8 (5)	-0.1 (5)
C(3A')	12 (1)	6.3 (8)	7.6 (7)	-1.0 (7)	0.7 (7)	-2.3 (6)
C(3B')	12 (1)	9 (1)	7.9 (8)	-4.3 (8)	-1.2 (7)	-1.4 (7)

^a The anisotropic thermal parameter is defined by the following expression: $\exp[-2\pi^2(U_{11}h^2a^{*2} + U_{22}k^2b^{*2} + U_{33}l^2c^{*2} + 2U_{12}hka^*b^* + 2U_{13}hla^*c^* + 2U_{23}klb^*c^*)]$. All hydrogen atoms were assigned a fixed isotropic temperature factor of $U = 0.0633 \text{ \AA}^2$.

The structure was solved by direct methods using the program MULTAN.²² Normalized structure factor amplitudes, $|E(hkl)|$, were generated from $|F_o(hkl)|$ values. The statistical distribution of $|E|$ values was consistent with that expected for a centrosymmetric crystal. The origin of the unit cell was defined by assigning zero phases to three strong reflections of appropriate parity (077, $|E| = 2.50$; 1,6,-5, $|E| = 4.47$; 681, $|E| = 2.12$). Four additional strong reflections of differing parity (468, $|E| = 2.70$; 4,10,-3, $|E| = 3.09$; 682, $|E| = 3.37$; 7,2,-4, $|E| = 2.91$) and many Σ_2 interactions were included in the starting reflection set. Application of the tangent formula by MULTAN generated phases for 496 reflections with $|E| > 1.63$. Assignments of real (0° or 180°) phases to the starting reflections provided 16 solutions. An E map generated from the phase set with the best combined figure of merit (2.82) yielded a chemically reasonable solution from which the coordinates of the phosphorus and sulfur atoms could be ascertained. A structure factor calculation based on these atomic sites and assuming an overall temperature factor of 2.5 \AA^2 gave $R_F = 30.8\%$ for all 3339 significant structure factor amplitudes. Subsequent Fourier syntheses revealed the locations of all remaining nonhydrogen atoms in the structure.

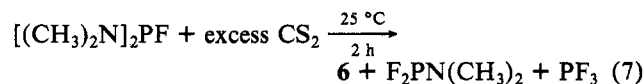
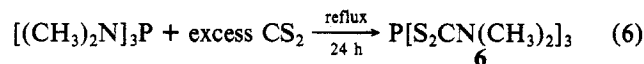
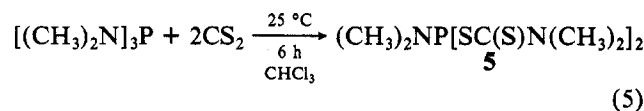
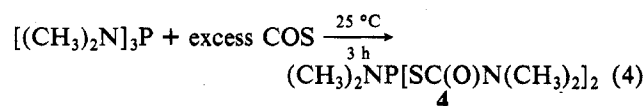
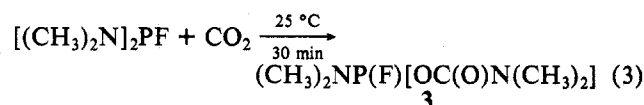
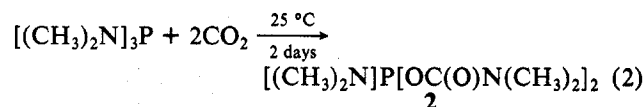
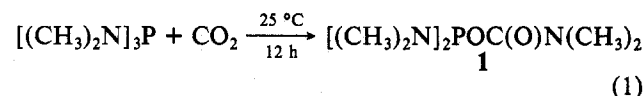
Refinement of the positional and individual isotropic thermal parameters of the nonhydrogen atoms by means of a block-diagonal least-squares procedure using counter weights, where $w = [\sigma_F^2 +$

$(CF_o)^2]^{-1}$ with $C = 0.06$, gave convergence at $R_F = 10.2\%$. At this point the coordinates of the 36 methyl hydrogen atoms were calculated in idealized positions, and all data were transferred to the X-RAY 76 system.²³

Individual anisotropic thermal parameters were then assumed for all nonhydrogen atoms. Several cycles of full-matrix least-squares refinement were then carried out in which the positions of all hydrogen atoms were fixed while the positional and anisotropic thermal parameters on the nonhydrogen atoms were varied. The coordinates of the 36 hydrogen atoms were then recalculated in idealized positions, and the process of full-matrix least-squares refinement was repeated with convergence after two cycles. The final values of R_F , R_{wF} , and GOF were 6.6%, 10.1%, and 1.2066, respectively. A final difference Fourier synthesis revealed no unusual features with the highest peak being 0.54 e \AA^{-3} at 0.125, 0.953, 0.313. A table of observed and calculated structure factor amplitudes is available.²⁴ Positional parameters are collected in Table II, and thermal parameters are listed in Table III.

Results and Discussion

In the present study the reactions of $[(\text{CH}_3)_2\text{N}]_3\text{P}$, $[(\text{CH}_3)_2\text{N}]_2\text{PF}$, $[(\text{CH}_3)_2\text{N}]_2\text{PCl}$, $\text{CH}_3\text{NCH}_2\text{CH}_2\text{N}(\text{CH}_3)\text{PF}$, $(\text{CH}_3)_2\text{NPF}_2$, and $(\text{CH}_3)_2\text{NPCl}_2$ with CO_2 , COS , and CS_2 in 1:1, 1:2, and 1:excess molar ratios have been examined in the absence of solvent. $[(\text{CH}_3)_2\text{N}]_2\text{PCl}$, $\text{CH}_3\text{NCH}_2\text{CH}_2\text{N}(\text{CH}_3)\text{PF}$, $(\text{CH}_3)_2\text{NPF}_2$, and $(\text{CH}_3)_2\text{NPCl}_2$ were found to be unreactive under all conditions employed: 400–1500 torr, 25–100 $^\circ\text{C}$. $[(\text{CH}_3)_2\text{N}]_3\text{P}$ and $[(\text{CH}_3)_2\text{N}]_2\text{PF}$, on the other hand, combine with CO_2 , COS , and CS_2 , and the reactions are summarized in eq 1–7. In each case the reactions lead



to the formation of P–N bond insertion products which have been identified by mass, infrared, and multinuclear NMR data. Attempts to prepare and isolate the 1:1 insertion products

(22) Germain, G.; Main, P.; Woolfson, M. M. *Acta Crystallogr., Sect. A* 1971, A27, 368.

(23) Stewart, J. M. "The X-ray 76 System", Technical Report TR-446; Computer Science Center, University of Maryland: College Park, MD, 1976.

(24) Supplementary material.

$[(\text{CH}_3)_2\text{N}]_2\text{P}[\text{SC}(\text{O})\text{N}(\text{CH}_3)_2]$, $[(\text{CH}_3)_2\text{N}]\text{P}(\text{F})[\text{SC}(\text{O})\text{N}(\text{C}-\text{H}_3)_2]$, $[(\text{CH}_3)_2\text{N}]_2\text{P}[\text{SC}(\text{S})\text{N}(\text{CH}_3)_2]$, and $[(\text{CH}_3)_2\text{N}]\text{P}(\text{F})[\text{SC}(\text{S})\text{N}(\text{CH}_3)_2]$, the 1:2 insertion products $[(\text{CH}_3)_2\text{N}(\text{O})\text{CO}]_2\text{PF}$ and $[(\text{CH}_3)_2\text{N}(\text{S})\text{CS}]_2\text{PF}$, and the 1:3 insertion products $[(\text{CH}_3)_2\text{N}(\text{O})\text{CO}]_3\text{P}$ and $[(\text{CH}_3)_2\text{N}(\text{O})\text{CS}]_3\text{P}$ or the respective short-lived transient species were unsuccessful. The combination of $[(\text{CH}_3)_2\text{N}]_3\text{P}$ and COS led to the only isolable COS insertion product, and the combinations of $[(\text{CH}_3)_2\text{N}]_2\text{PF}$ with COS or CS_2 led to rearrangement products. Compound **3** represents the first isolated example of a carbamate complex of an aminohalophosphine. At 25 °C, **3** is unstable toward disproportionation to **2** and $\text{F}_2\text{PN}(\text{CH}_3)_2$ (half-life ≈ 48 h); however, **3** is indefinitely stable at -78 °C.

Mass Spectra. The mass spectra of **1–6** are complex and several ion assignments are ambiguous since loss of either CO_2 or $\text{N}(\text{CH}_3)_2$ fragments accounts for 44 mass units. Compounds **1** and **3** show parent ions and fragmentation patterns which support the proposed compositions. The highest mass ion observed for **2** appears at m/e 207, which corresponds to loss of CO_2 from the parent ion.²⁵ The mass spectrum of **4** is closely related to that of **2**; the parent ion is unobserved and the highest mass ion, m/e 223, corresponds to (parent ion – COS)⁺. The sequential loss of COS and $\text{N}(\text{CH}_3)_2$ fragments is clearly distinguished. The parent ions for **5** and **6** are unobserved, and the spectra are dominated by rearrangement ions.²⁶ Ions characteristic of the dithiocarbamate group are observed at m/e 121 and 88.

Infrared Spectra. The infrared spectra of **1–4** are closely related, and several tentative vibrational mode assignments are possible;^{15d,27,28} 2920–2790, 1700–1670, 1490–1270, 1190–1160, 990–890, 800–700, and 700–650 cm^{-1} are tentatively assigned to C–H stretching, C=O stretching, CH_3 deformation, P–O–C stretching, $(\text{CH}_3)_2\text{N–P}$ stretching, P–F stretching and N–P(N)F stretching modes, respectively. Although every band has not been assigned, it is clear that there remains at least one P–N bond in **1–4** which has not undergone insertion. The strong carbonyl absorption bands at 1693 (**1**), 1682 (**2**), 1696 (**3**), and 1657 and 1642 cm^{-1} (**4**) suggest that monodentate $\text{POC}(\text{O})\text{NMe}_2$ and $\text{PSC}(\text{O})\text{NMe}_2$ coordination complexes have been formed.

The infrared spectra of **5** and **6** are distinct from the spectra of **1–4**. In particular, the carbamate carbonyl band is absent. A P–N stretching mode at 670 cm^{-1} in **5** is not present in **6**, which suggests that each of the three P–N bonds has undergone insertion by CS_2 . Bands in the region 1290–1130 cm^{-1} are attributed to the dithiocarbamate group;²⁸ however, overlap with other ligand modes precludes an unambiguous assignment. The bands at 1485 cm^{-1} , **5**, and 1495 cm^{-1} , **6**, may be assigned to a stretching mode for the polar ligand resonance form $\text{S}_2=\text{C}=\text{N}^+\text{R}_2$.^{28,29}

NMR Spectra.³⁰ The NMR spectra of **1–3** are related, and they are consistent with the formation of monodentate carbamate groups bonded to the central pyramidal phosphorus

atom. The $^{31}\text{P}\{^1\text{H}\}$ spectra (neat) show singlets centered at 129.3 ppm in **1** and 128.3 ppm in **2**. A doublet centered at 137.4 ppm, $J_{\text{PF}} = 1137$ Hz, is observed in **3**. Restoration of $^1\text{H–}^{31}\text{P}$ coupling reveals a nine-line multiplet with intensities corresponding to a thirteen-line multiplet in **1**, $^3J_{\text{PNCH}} = 10.5$ Hz, a septet in **2**, $J_{\text{PNCH}} = 9.7$ Hz, and a doublet of septets in **3**, $^3J_{\text{PNCH}} = 9.3$ Hz. Phosphorus-31 chemical shifts are known to be sensitive to coordination number,^{31–33} and the correlation is demonstrated in the phosphorane carbamate $\text{CH}_3(\text{CF}_3)_3\text{P}[\text{O}_2\text{CN}(\text{CH}_3)_2]$ (**7**) prepared by Cavell and co-workers.¹⁴ The crystal structure of **7** shows that the carbamate group is bidentate and that the phosphorus atom is six-coordinate. Correspondingly, the ^{31}P chemical shift, -139 ppm, falls in the region normally associated with six-coordinate phosphorane complexes. In **1–3** the chemical shifts appear in the region for tricoordinate aminophosphines;^{31–33} therefore, monodentate carbamate coordination is inferred. In **1** and **2** the shifts are slightly downfield from that of $\text{P}[\text{N}(\text{CH}_3)_2]_3$, as would be expected from electronegativity effects,³⁴ while the shift for **3** is unexpectedly upfield from that of $\text{P}[\text{N}(\text{C–H}_3)_2]_3$. The multiplets observed in the ^1H -coupled spectra result from coupling of the phosphorus atom with the methyl protons on the intact P– $\text{N}(\text{CH}_3)_2$ groups.

The ^1H NMR spectra (neat) show a sharp, high-field doublet and a broad low-field resonance: **1**, $\delta(\text{H}_a)$ 2.35 ($^3J_{\text{HCNP}} = 10.5$ Hz, area 2), $\delta(\text{H}_b)$ 2.70 (area 1); **2**, $\delta(\text{H}_a)$ 2.48 ($^3J_{\text{HCNP}} = 10.0$ Hz, area 1), $\delta(\text{H}_b)$ 2.72 (area 2); **3**, $\delta(\text{H}_a)$ 2.36 ($^3J_{\text{HCNP}} = 9.5$ Hz, $^4J_{\text{HCNPF}} = 3.5$ Hz, area 1), $\delta(\text{H}_{b,c})$ 2.56 (area 1). The downfield shift, area ratios, and loss of resolvable J_{HCNP} coupling³⁵ in the low-field resonance are diagnostic of CO_2 insertion in one or more PN bonds. The $^{13}\text{C}\{^1\text{H}\}$ NMR spectrum (neat) for **1** shows a methyl doublet $\delta(\text{C}_a)$ 37.59 ($^2J_{\text{CNP}} = 18.5$ Hz) and a broad methyl singlet $\delta(\text{C}_b)$ 36.53. These resonances are assigned to the methyl carbon atoms on the intact amide groups and the carbamate methyl carbon atoms, respectively. The central carbamate carbon atom was not detected. The spectrum for **2** shows a methyl doublet $\delta(\text{C}_a)$ 36.13 ($^2J_{\text{CNP}} = 34.7$ Hz), a broad methyl singlet $\delta(\text{C}_b)$ 36.35, and a low-field carbonyl doublet $\delta(\text{C}_c)$ 154.06 ($^2J_{\text{COP}} = 8.7$ Hz). The spectrum of **3** shows a methyl doublet of doublets $\delta(\text{C}_a)$ 34.29 ($^2J_{\text{CNP}} = 23.2$ Hz, $^3J_{\text{CNPF}} = 2.6$ Hz), two methyl group singlets $\delta(\text{C}_b)$ 35.75 and $\delta(\text{C}_c)$ 36.18, and a low-field carbonyl doublet of doublets $\delta(\text{C}_d)$ 153.58 ($^2J_{\text{COP}} = 7.5$ Hz, $^3J_{\text{COPF}} = 3.2$ Hz). In **3** the carbon atoms C_b and C_c belong to nonequivalent methyl groups on the monodentate carbamate group.

The NMR spectra for the carbonyl sulfide and carbon disulfide insertion products, **4–6**, are related. The $^{31}\text{P}\{^1\text{H}\}$ spectra (CHCl_3) show a singlet centered at 84.0, 60.1, and -62.6 ppm, respectively. Restoration of $^1\text{H–}^{31}\text{P}$ coupling results in a seven-line multiplet in **4**, $^3J_{\text{HCNP}} = 10.0$ Hz, but this coupling is not observed in **5** or **6**. The chemical shifts for **4** and **5** occur in the range for tricoordinate phosphines, and monodentate thiocarbamate coordination is implied.³⁶ By comparison with the shift for $\text{P}[\text{N}(\text{CH}_3)_2]_3$,³⁰ the very high-field shift observed for **6** suggests a dramatic increase in

- (25) Initial loss of CO_2 instead of $\text{N}(\text{CH}_3)_2$ upon electron impact of **2** is assumed since the initial loss of COS from **4** is unambiguous. Elimination of CO_2 upon electron impact is also found for compounds of the general type $\text{ROC}(\text{O})\text{OR}$, $\text{ROC}(\text{O})\text{SR}$, $\text{ArC}(\text{O})\text{OC}(\text{CH}_3)_3$, and $\text{ArOC}(\text{O})\text{C}(\text{CH}_3)_3$; McLafferty, F. W. "Interpretation of Mass Spectra"; W. A. Benjamin: New York, 1973.
- (26) Phosphorus-sulfur compounds are typically subjected to extensive structural rearrangement upon electron impact, and the compositions of **5** and **6** must be deduced from chemical analyses: Granth, I. Top. Phosphorus Chem. 1976, 8, 41.
- (27) Corbridge, D. E. C. Top. Phosphorus Chem. 1969, 6, 235.
- (28) Shankaranarayana, M. L.; Patel, C. C. Spectrochim. Acta 1965, 21, 95.
- (29) Colton, R.; Levitus, R.; Wilkinson, G. J. Chem. Soc. 1960, 5275. Chatt, J.; Duncanson, L. A.; Venanzi, L. M. Nature (London) 1956, 177, 1042.
- (30) The NMR spectra for the free ligands provide the following parameters: $[(\text{CH}_3)_2\text{N}]_3\text{P}$, $^{31}\text{P}\{^1\text{H}\}$ δ 122.0, ^1H δ 2.50 ($^3J_{\text{HCNP}} = 9.0$ Hz), $^{13}\text{C}\{^1\text{H}\}$ δ 38.96 ($^2J_{\text{CNP}} = 19.0$ Hz); $[(\text{CH}_3)_2\text{N}]_2\text{PF}$, $^{31}\text{P}\{^1\text{H}\}$ δ 150.9 ($^1J_{\text{PF}} = 1038$ Hz), ^1H δ 2.42 ($^3J_{\text{HCNP}} = 7$ Hz, $^4J_{\text{HCNPF}} = 3$ Hz), $^{13}\text{C}\{^1\text{H}\}$ δ 35.9 ($^2J_{\text{CNP}} = 19.0$ Hz, $^3J_{\text{CNPF}} = 2.0$ Hz).

- (31) Nixon, J. F.; Schmutzler, R. Spectrochim. Acta 1964, 20, 1835.
- (32) Mark, V.; Dungan, C. H.; Crutchfield, M. M.; Van Wazer, J. R. Top. Phosphorus Chem. 1967, 5, 1.
- (33) Thomas, M. G.; Schultz, C. W.; Parry, R. W. Inorg. Chem. 1977, 16, 994.
- (34) Van Wazer, J. R.; Callis, C. F.; Scholery, J. N.; Jones, R. C. J. Am. Chem. Soc. 1956, 78, 5715. Estimates of the ^{31}P chemical shifts: **1**, 129 ppm; **2**, 136 ppm.
- (35) The proton resonances for the $\text{POC}(\text{O})\text{N}(\text{CH}_3)_2$ group may appear broadened (~ 10 Hz) as a result of unresolved $^1\text{H–}^{31}\text{P}$ coupling or inequivalent cis and trans methyl group environments.
- (36) Estimates³⁴ for the chemical shifts of **4** and **5** on the assumption of monodentate thiocarbamate connectivities $>\text{PSC}(\text{O})\text{N}(\text{CH}_3)_2$ and $>\text{PSC}(\text{S})\text{N}(\text{CH}_3)_2$, respectively, are 72 and 66 ppm. If a $\text{POC}(\text{S})\text{N}(\text{CH}_3)_2$ connectivity is assumed for **4**, the calculated shift is 136 ppm.

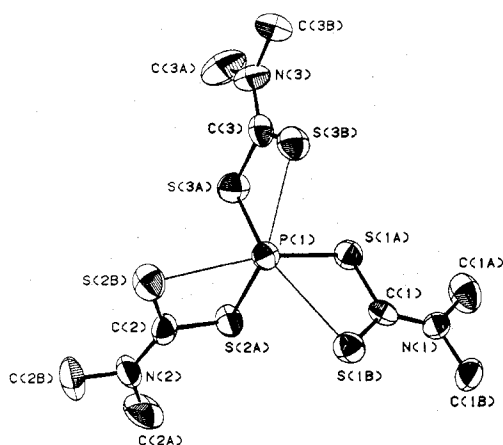


Figure 1. Molecular geometry and labeling of atoms in the $P[S_2CN(CH_3)_2]_3$ molecule A (50% probability ellipsoids).

phosphorus atom coordination number.³⁷

The 1H NMR spectra ($CHCl_3$) in the methyl region show a sharp high-field doublet and broad low-field singlet for **4** and **5** and a single resonance for **6**: **4**, $\delta(H_a)$ 2.82 ($^3J_{HCNP} = 10.0$ Hz, area 1), $\delta(H_b)$ 3.07 (area 2); **5**, $\delta(H_a)$ 2.76 ($^3J_{HCNP} = 8.5$ Hz, area 1), $\delta(H_b)$ 3.44 (area 2); **6**, $\delta(H)$ 3.51. The $^{13}C\{^1H\}$ NMR spectrum of **4** shows a methyl doublet $\delta(C_a)$ 40.84 ($^2J_{CNP} = 16.0$ Hz), two methyl singlets $\delta(C_b)$ 39.10 and $\delta(C_c)$ 37.66, and a carbonyl doublet $\delta(C_d)$ 167.36 ($^2J_{CSP} = 17.0$ Hz). The spectrum of **5** shows a methyl doublet $\delta(C_a)$ 41.75 ($^2J_{CNP} = 10.2$ Hz), two methyl singlets $\delta(C_b)$ 45.30 and $\delta(C_c)$ 43.67, and a carbonyl doublet $\delta(C_d)$ 196.76 ($^2J_{CSP} = 27.9$ Hz). The spectrum of **6** shows a methyl singlet $\delta(C_a)$ 44.51 and a thiocarbonyl doublet $\delta(C_b)$ 196.74 ($^2J_{CSP} = 21.8$ Hz). The appearance of two methyl-group environments in the $^{13}C\{^1H\}$ NMR spectra for the carbamate groups on **3**, **4**, and **5** suggests that rotation about the monodentate $-C(X)-NR_2$ bond is severely restricted at 30 °C.

Characterization data previously collected for phosphine carbamate and thiocarbamate complexes have not provided a complete definition of the potential monodentate-bidentate linkage isomerization. The infrared and NMR data presented here clearly support the assignment of monodentate carbamate and thiocarbamate coordination geometries for **1–5**, and there is no evidence indicating the existence of bidentate isomers. The monodentate coordination contrasts with the bidentate coordination found by Cavell for the aminophosphorane insertion compounds $CH_3(CF_3)_3PO_2CN(CH_3)_2$, $CH_3(CF_3)_3PO-SCN(CH_3)_2$, and $CH_3(CF_3)_3PS_2CN(CH_3)_2$.¹⁴ The infrared and NMR characterization data for **6**, on the other hand, do not provide a clear structural assignment. The spectroscopic data are consistent with the formation of bidentate dithiocarbamate linkages at the central phosphorus atom, but a combination of monodentate and bidentate coordination or a dynamic linkage isomerization process cannot be excluded. This ambiguity prompted the determination of the solid-state molecular structure of **6** by single-crystal X-ray diffraction methods.

Crystal Structure. The results of the X-ray analysis confirm the formulation of **6** as $[(CH_3)_2NCS]_3P$. The structure contains discrete monomeric molecules with eight molecules per unit cell and two independent molecules (A and B) per asymmetric unit. For each molecule there are two optically active isomers which form a racemic mixture in the crystal.

Table IV. Bond Distances (Å) and Their Esd's for $P[S_2CN(CH_3)_2]_3$

(A) Phosphorus-Sulfur Bond Lengths			
P(1)-S(1A)	2.202 (3)	P(1')-S(1A')	2.180 (3)
P(1)-S(2A)	2.181 (3)	P(1')-S(2A')	2.173 (3)
P(1)-S(3A)	2.162 (3)	P(1')-S(3A')	2.167 (3)
P(1)-S(1B)	3.016 (3)	P(1')-S(1B')	3.014 (3)
P(1)-S(2B)	2.873 (3)	P(1')-S(2B')	2.982 (3)
P(1)-S(3B)	2.936 (3)	P(1')-S(3B')	2.973 (3)

(B) Sulfur-Carbon Bond Lengths			
S(1A)-C(1)	1.752 (8)	S(1A')-C(1')	1.774 (8)
S(2A)-C(2)	1.756 (8)	S(2A')-C(2')	1.752 (8)
S(3A)-C(3)	1.776 (8)	S(3A')-C(3')	1.766 (9)
S(1B)-C(1)	1.676 (8)	S(1B')-C(1')	1.663 (8)
S(2B)-C(2)	1.676 (8)	S(2B')-C(2')	1.670 (8)
S(3B)-C(3)	1.651 (8)	S(3B')-C(3')	1.661 (9)

(C) (S-Bonded) Carbon-Nitrogen Bond Lengths			
C(1)-N(1)	1.32 (1)	C(1')-N(1')	1.32 (1)
C(2)-N(2)	1.33 (1)	C(2')-N(2')	1.34 (1)
C(3)-N(3)	1.34 (1)	C(3')-N(3')	1.33 (1)

(D) Nitrogen-Carbon (Methyl) Bond Lengths			
N(1)-C(1A)	1.47 (1)	N(1')-C(1A')	1.47 (1)
N(1)-C(1B)	1.47 (1)	N(1')-C(1B')	1.46 (1)
N(2)-C(2A)	1.47 (1)	N(2')-C(2A')	1.42 (1)
N(2)-C(2B)	1.46 (1)	N(2')-C(2B')	1.48 (1)
N(3)-C(3A)	1.47 (1)	N(3')-C(3A')	1.47 (1)
N(3)-C(3B)	1.42 (1)	N(3')-C(3B')	1.44 (2)

Table V. Bond Angles (Deg) and Their Esd's for $P[S_2CN(CH_3)_2]_3$

(A) Angles within PS_6 Core			
S(1A)-P(1)-S(1B)	67.5 (1)	S(1A')-P(1')-S(1B')	67.7 (1)
S(2A)-P(1)-S(2B)	70.2 (1)	S(2A')-P(1')-S(2B')	68.4 (1)
S(3A)-P(1)-S(3B)	69.6 (1)	S(3A')-P(1')-S(3B')	68.6 (1)
S(1A)-P(1)-S(2A)	91.4 (1)	S(1A')-P(1')-S(2A')	92.0 (1)
S(2A)-P(1)-S(3A)	91.1 (1)	S(2A')-P(1')-S(3A')	90.6 (1)
S(3A)-P(1)-S(1A)	89.3 (1)	S(3A')-P(1')-S(1A')	91.0 (1)
S(1A)-P(1)-S(2B)	161.6 (1)	S(1A')-P(1')-S(2B')	159.8 (1)
S(2A)-P(1)-S(3B)	160.5 (1)	S(2A')-P(1')-S(3B')	159.2 (1)
S(3A)-P(1)-S(1B)	156.6 (1)	S(3A')-P(1')-S(1B')	158.1 (1)
S(1A)-P(1)-S(3B)	91.0 (1)	S(1A')-P(1')-S(3B')	88.6 (1)
S(2A)-P(1)-S(1B)	86.5 (1)	S(2A')-P(1')-S(1B')	85.6 (1)
S(3A)-P(1)-S(2B)	90.4 (1)	S(3A')-P(1')-S(2B')	94.2 (1)
S(1B)-P(1)-S(2B)	110.5 (1)	S(1B')-P(1')-S(2B')	104.3 (1)
S(2B)-P(1)-S(3B)	106.1 (1)	S(2B')-P(1')-S(3B')	111.5 (1)
S(3B)-P(1)-S(1B)	112.2 (1)	S(3B')-P(1')-S(1B')	113.7 (1)

(B) P-S-C Angles			
P(1)-S(1A)-C(1)	98.4 (3)	P(1')-S(1A')-C(1')	98.6 (3)
P(1)-S(1B)-C(1)	73.6 (3)	P(1')-S(1B')-C(1')	73.8 (3)
P(1)-S(2A)-C(2)	95.2 (3)	P(1')-S(2A')-C(2')	97.4 (3)
P(1)-S(2B)-C(2)	74.8 (3)	P(1')-S(2B')-C(2')	73.0 (3)
P(1)-S(3A)-C(3)	96.0 (3)	P(1')-S(3A')-C(3')	97.5 (3)
P(1)-S(3B)-C(3)	73.7 (3)	P(1')-S(3B')-C(3')	73.6 (3)

(C) Angles in Ligand 1			
S(1A)-C(1)-S(1B)	120.5 (5)	S(1A')-C(1')-S(1B')	119.9 (5)
S(1A)-C(1)-N(1)	115.2 (6)	S(1A')-C(1')-N(1')	115.0 (6)
S(1B)-C(1)-N(1)	124.2 (6)	S(1B')-C(1')-N(1')	125.1 (6)
C(1)-N(1)-C(1A)	120.3 (7)	C(1')-N(1')-C(1A')	123.8 (7)
C(1)-N(1)-C(1B)	123.1 (7)	C(1')-N(1')-C(1B')	120.5 (7)
C(1A)-N(1)-C(1B)	116.5 (7)	C(1A')-N(1')-C(1B')	115.7 (7)

(D) Angles in Ligand 2			
S(2A)-C(2)-S(2B)	119.2 (5)	S(2A')-C(2')-S(2B')	120.7 (5)
S(2A)-C(2)-N(2)	116.6 (6)	S(2A')-C(2')-N(2')	114.4 (6)
S(2B)-C(2)-N(2)	124.2 (6)	S(2B')-C(2')-N(2')	124.9 (6)
C(2)-N(2)-C(2A)	122.9 (7)	C(2')-N(2')-C(2A')	124.0 (8)
C(2)-N(2)-C(2B)	119.9 (7)	C(2')-N(2')-C(2B')	120.5 (7)
C(2A)-N(2)-C(2B)	117.2 (8)	C(2A')-N(2')-C(2B')	115.4 (7)

(E) Angles in Ligand 3			
S(3A)-C(3)-S(3B)	120.6 (5)	S(3A')-C(3')-S(3B')	120.3 (5)
S(3A)-C(3)-N(3)	114.3 (6)	S(3A')-C(3')-N(3')	115.4 (7)
S(3B)-C(3)-N(3)	125.1 (7)	S(3B')-C(3')-N(3')	124.2 (7)
C(3)-N(3)-C(3A)	123.7 (8)	C(3')-N(3')-C(3A')	122.3 (8)
C(3)-N(3)-C(3B)	119.4 (8)	C(3')-N(3')-C(3B')	122.3 (9)
C(3A)-N(3)-C(3B)	116.7 (8)	C(3A')-N(3')-C(3B')	115.3 (8)

(37) ^{31}P chemical shift data for phosphines with five or six sulfur atoms as substituents are not available for comparison, and it remains unclear what magnitude the calculated shift for these coordination geometries should be.

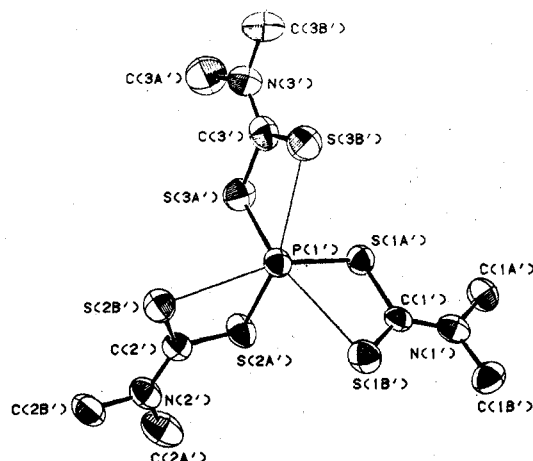


Figure 2. Molecular geometry and labeling of atoms in the $P[S_2C-N(CH_3)_2]_3$ molecule B (50% probability ellipsoids).

Table VI. Average Bond Distances (Å) and Angles (Deg)^a with Their Esd's for

$P \begin{bmatrix} S(\alpha) \\ S(\beta) \end{bmatrix} C - N \begin{bmatrix} C(\alpha) \\ C(\beta) \end{bmatrix}_3$			
Bond Distances			
P-S(α)	2.178 ± 0.009	C-N	1.33 ± 0.01
P-S(β)	2.966 ± 0.031	N-C(α)	1.46 ± 0.01
S(α)-C	1.763 ± 0.004	N-C(β)	1.46 ± 0.01
S(β)-C	1.666 ± 0.005		
Bond Angles			
S(α)-P-S(β)	68.7 ± 0.6	S(β)-C-N	124.6 ± 0.1
P-S(α)-C	97.2 ± 0.7	C-N-C(α)	122.8 ± 0.8
P-S(β)-C	73.8 ± 0.4	C-N-C(β)	121.0 ± 0.6
S(α)-C-S(β)	120.2 ± 0.3	C(α)-N-C(β)	116.1 ± 0.3
S(α)-C-N	115.2 ± 0.5		

^a Esd's on average value as preceded by "±" are calculated by the formula $\sigma = [\sum(d_i - d)^2 / (N - 1)]^{1/2}$.

The three dithiocarbamate ligands bonded to the central phosphorus atom act as bidentate ligands, and the resulting PS_6 polyhedron approximates a distorted trigonal antiprism or distorted capped octahedron. Figures 1 and 2 show labeled drawings of A and B. Selected bond lengths, angles, and averaged bond lengths and bond angles are summarized in Tables IV–VI.

The structure of the PS_6 polyhedron is similar to the structure of the AsS_6 polyhedron in the related complex $[(C_2H_5)_2NCS_2]_3As$.¹² In 6 each four-membered chelate ring contains a short and a long P–S distance. The average short P–S(α) distance, 2.178 (9) Å, is less than the average short As–S distance, 2.348 (11) Å; however, the average long P–S(β) distance, 2.966 (31) Å, in 6 is greater than the average long As–S distance, 2.841 (54) Å. The short P–S(α) bond distances can be assigned to typical covalent overlaps,³⁸ and the trend in bond lengthening from phosphorus to arsenic is consistent with the smaller covalent radius for the phosphorus atom. The long P–S(β) bond distances may be considered to be weak ionic interactions of the type P^+-S^- . It might be expected that the P^+-S^- interactions would be weaker in 6 than the As^+-S^- interactions in $[(C_2H_5)_2NCS_2]_3As$ due to the smaller ionic radius of 6 and the steric crowding imposed by the three covalently bonded sulfur atoms. The longer P–S(β) bond distances in 6 support this suggestion. The average internal

Table VII. S–S Nonbonded Distances (Å)

molecule A		molecule B	
Site Distances			
S(1A)–S(1B)	2.977 (3)	S(1A')–S(1B')	2.974
S(2A)–S(2B)	2.960 (3)	S(2A')–S(2B')	2.975
S(3A)–S(3B)	2.977 (3)	S(3A')–S(3B')	2.973
Interligand Distances			
S(1A)–S(2A)	3.138 (3)	S(1A')–S(2A')	3.131 (3)
S(2A)–S(3A)	3.101 (3)	S(2A')–S(3A')	3.083 (3)
S(3A)–S(1A)	3.067 (3)	S(3A')–S(1A')	3.099 (3)
S(1B)–S(2B)	4.840 (4)	S(1B')–S(2B')	4.735 (3)
S(2B)–S(3B)	4.642 (4)	S(2B')–S(3B')	4.924 (4)
S(3B)–S(1B)	4.941 (3)	S(3B')–S(1B')	5.014 (4)

Table VIII. Least-Squares Planes,^a Atomic Deviations from the Planes, and Angles of Intersecting Planes

Planes and Deviations (Å)			
atom	dev	atom	dev
Molecule A			
Plane I: $0.9796I - 0.1492J + 0.1344K = 4.3256$			
P(1)	0.012	N(1)	–0.009
C(1)	–0.002	C(1A)	0.039
S(1A)	0.016	C(1B)	–0.025
S(1B)	–0.031		
Plane II: $0.3918I + 0.5056J - 0.7687K = 5.2423$			
P(1)	–0.114	N(2)	–0.028
C(2)	0.035	C(2A)	–0.060
S(2A)	0.134	C(2B)	–0.001
S(2B)	0.040		
Plane III: $0.0320I + 0.7811J + 0.6235K = 10.2101$			
P(1)	0.071	N(3)	–0.021
C(3)	–0.025	C(3A)	0.007
S(3A)	–0.043	C(3B)	0.063
S(3B)	–0.053		
Molecule B			
Plane IV: $0.9811I + 0.1598J + 0.1094K = 5.8792$			
P(1')	0.018	N(1')	0.011
C(1')	–0.009	C(1A')	0.023
S(1A')	–0.035	C(1B')	–0.015
S(1B')	0.007		
Plane V: $-0.3634I + 0.5647J + 0.7409K = 2.4070$			
P(1')	–0.094	N(2')	–0.023
C(2')	0.025	C(2A')	–0.031
S(2A')	0.101	C(2B')	–0.023
S(2B')	0.045		
Plane VI: $-0.1207I + 0.7260J - 0.6770K = -0.9278$			
P(1')	–0.031	N(3')	–0.016
C(3')	0.035	C(3A')	–0.051
S(3A')	0.058	C(3B')	0.029
S(3B')	–0.025		

Plane Angles, Deg

molecule A		molecule B	
planes	angle	planes	angle
I–II	78.2	II–III	85.9
I–III	89.9	IV–V	79.3
		V–VI	87.3
		IV–VI	85.6

^a The equations of the planes are expressed as $PI + QJ + Rk = S$ in orthogonal angstrom space.

chelate ring angles S(α)–P–S(β), 68.7 (6)°, and S(α)–C–S(β), 120.2 (3)°, in 6 are respectively smaller and larger than the similar angles in the arsenic analogue, (S–As–S)_{av} = 90.16°, and typical transition-metal tris(1,1-dithiolates), S–M–S = 72–78° and S–C–S = 108–115°. The average P–S(α)–C

(38) Pauling, L. "The Nature of the Chemical Bond", 3rd ed.; Cornell University Press: Ithaca, NY, 1960.

(39) Eisenberg, R. *Prog. Inorg. Chem.* 1970, 12, 295.

and P-S(β)-C chelate angles in **6** also are noticeably dissimilar.

The nonbonded sulfur-sulfur distances are summarized in Table VII. The average intraligand "bite" distance is 2.97 Å, which is longer than the "bite" distance in many metal-1,1-dithiolato complexes³⁹ yet shorter than the S-S van der Waals contact distance of 3.4 Å.⁴⁰ The three sulfur atoms, S(α), covalently bonded to the phosphorus atom form a triangle with nonbonded edge distances in the range 3.067-3.138 Å in A and 3.083-3.131 Å in B. The three ionically associated sulfur atoms, S(β), form a triangle with nonbonded edge distances in the ranges 4.642-4.941 Å in A and 4.735-5.014 Å in B. The two triangles are rotated by about 45° in each molecule and the triangular S₃ planes are out of parallel by 2.9° in A and 4.0° in B.

The overall distortions in the PS₆ coordination polyhedron away from octahedral symmetry are indicated by the unequal P-S bond distances, the S-P-S and dithiocarbamate ligand bond angles, the trigonal S₃ face twist, and the large volume of coordination space between the S(β) atoms. These distortions appear to result from a combination of steric constraints imposed by the tris(dithiocarbamate) chelate structure and a balance of covalent and ionic P-S electrostatic attractions. Nonbonded S-S and S-P lone-pair van der Waals repulsions also play some role in determining the final configuration.

The geometry of the individual dithiocarbamate ligands is also of interest. The average S(α)-C distance, 1.763 Å, is significantly longer than the average S(β)-C distance, 1.666

Å, and a comparable effect is also observed in the arsenic complex: S(α)-C = 1.760 Å and S(β)-C = 1.678 Å. The average C-N bond distance, 1.33 Å, is comparable with those of most 1,1-dithiolato complexes.^{39,41} The two sulfur atoms, two nitrogen atoms, and three carbon atoms of each ligand form a plane which contains the central phosphorus atom. The equations for these planes and the atom deviations from the planes are summarized in Table VIII. The small distortions from planarity are likely a result of crystal-packing forces. The angles between the three ligand propeller blades, 78.2, 85.9, and 89.9° in A and 79.3, 85.6, and 87.3° in B, deviate from the 90° angle expected for an octahedral complex. Planes calculated for the CS₂ and NC₂ portions of each chelate ring show very small torsion angles in the S₂C-NC₂ linkage, 1.9-4.2°.

Acknowledgment. The authors wish to recognize NSF Grants CHE-7802921 and MPS75-06111, which facilitated the purchases of the X-ray diffractometer and the NMR data system. R.T.P. wishes to acknowledge partial support of this work by the UNM Research Allocations Committee.

Registry No. 1, 4175-80-8; 2, 75101-76-7; 3, 75101-77-8; 4, 75101-78-9; 5, 75101-79-0; 6, 75102-48-6; [(CH₃)₂N]₃P, 1608-26-0; FP[N(CH₃)₂]₂, 1735-82-6; CO₂, 124-38-9; COS, 463-58-1; CS₂, 75-15-0.

Supplementary Material Available: Tables of mass and infrared spectrometric data (4 pages) and a table of observed and final calculated structure factors (16 pages). Ordering information is given on any current masthead page.

(40) van der Helm, D.; Lessor, A. E.; Merritt, L. L. *Acta Crystallogr.* **1960**, *13*, 1050. Eisenberg, R.; Ibers, J. A. *J. Am. Chem. Soc.* **1965**, *87*, 3776; *Inorg. Chem.* **1966**, *5*, 411.

(41) The structure of Na[S₂CN(C₂H₅)₂]₂·3H₂O contains an ionic symmetrical dithiocarbamate ligand with C-S and C-N bond distances of 1.720 (7) and 1.344 (8) Å. Colapietro, M.; Domenicano, A.; Vacic, A. *Chem. Commun.* **1968**, 572.

Contribution from the Department of Chemistry, The Johns Hopkins University, Baltimore, Maryland 21218, the Department of Chemistry and Materials Science Center, Northwestern University, Evanston, Illinois 60201, and the National Bureau of Standards, Washington, D. C. 20234

Crystal and Molecular Structure of an Unusual Salt Formed from the Radical Cation of Tetrathiafulvalene (TTF) and the Trichloromercurate Anion (HgCl₃), (TTF)(HgCl₃)

T. J. KISTENMACHER,*^{1a} M. ROSSI,^{1a} C. C. CHIANG,^{1a} R. P. VAN DUYNE,^{1b} and A. R. SIEDLE*^{1c}

Received April 23, 1980

The synthesis and crystal structure of the salt (TTF)(HgCl₃) are reported. Crystals of the salt are triclinic, of space group *P* $\bar{1}$, with *a* = 12.661 (3) Å, *b* = 15.969 (4) Å, *c* = 7.416 (2) Å, α = 98.69 (2)°, β = 95.73 (2)°, γ = 120.01 (2)°, *V* = 1256.2 Å³, mol wt ((C₆H₄S₄)(HgCl₃)) = 511.3, *Z* = 4, *D*_{meas} = 2.68 (1) g cm⁻³, and *D*_{calcd} = 2.70 g cm⁻³. The structure was solved by standard Patterson and Fourier methods and has been refined by full-matrix least squares, based on 4298 counter-collected *F*_o's, to a final *R* value of 0.080. The structure can be qualitatively separated into two layers parallel to the *ac* plane. One of these layers, centered about *y* = 0.0, contains both inorganic and organic polymers propagating along the crystallographic *c* axis. The covalent inorganic polymer contains roughly trigonal-bipyramidal coordination about the Hg(II) center, with equatorial Hg-Cl bond lengths of 2.374 (5), 2.395 (5), and 2.545 (5) Å and considerably longer axial bond lengths of 2.982 (5) and 3.112 (5) Å. Collinear with this covalent inorganic polymer is a columnar array of stacked TTF radical cations. The stacking in this columnar array of TTF cations is nominally of the ring-over-bond type with a mean separation between planes of 3.6 Å. The second layer, centered about *y* = 0.5, contains solely dimeric species. The chloromercurate anion is a dimeric, edge-shared bitetrahedron, with Hg-Cl bond lengths of 2.600 (5) and 2.696 (5) Å for the bridging chloro ligands and 2.368 (5) and 2.381 (5) Å for the two independent terminal chloro ligands. The organic dimer is made up of two strongly associated and nearly eclipsed TTF cations, with a mean spacing of 3.43 Å. Resonance Raman data have been interpreted as suggesting the presence of two different kinds of TTF moieties, consistent with the X-ray data. From the Raman data it is indicated that the two different TTF species have slightly different degrees of charge transfer.

Introduction

The solid-state chemistry of a wide variety of low-dimensional materials containing tetrathiafulvalene (TTF) or tet-

racyno-*p*-quinodimethane (TCNQ) has received considerable attention in the past few years. A relatively large body of literature now exists on (TTF)(TCNQ), its derivatives and analogues, simple and associated halogen salts of TTF, and ammonium, alkali-metal, and alkaline-earth salts containing TCNQ.² Less attention has been paid to simple inorganic

(1) (a) The Johns Hopkins University. (b) Northwestern University. (c) National Bureau of Standards.